Available online at www.sciencedirect.com
SCIENCE DIRECT®
Journal of Solid State Chemistry 177 (2004) 883–888
JOURNAL OF SOLID STATE CHEMISTRY
http://elsevier.com/locate/jssc

Characterization of quasi-one-dimensional $S = 1/2$ Heisenberg antiferromagnets $Sr_2Cu(PO_4)_2$ and $Ba_2Cu(PO_4)_2$ with magnetic susceptibility, specific heat, and thermal analysis

A.A. Belik,[a,*] M. Azuma,[a,b] and M. Takano[a]

[a] *Institute for Chemical Research, Kyoto University, Gokasho, Uji, Kyoto-fu 611-0011, Japan*
[b] *PRESTO, Japan Science and Technology Corporation (JST), Kawaguchi, Saitama 332-0012, Japan*

Received 14 July 2003; received in revised form 28 August 2003; accepted 23 September 2003

Abstract

Properties of $Sr_2Cu(PO_4)_2$ and $Ba_2Cu(PO_4)_2$ having $[Cu(PO_4)_2]_\infty$ linear chains in their structures with Cu–O–P–O–Cu linkages were studied by magnetic susceptibility ($T = 2-400$ K, $H = 100$ Oe) and specific heat measurements ($T = 0.45-21$ K). Magnetic susceptibility versus temperature curves, $\chi(T)$, showed broad maxima at $T_M = 92$ K for $Sr_2Cu(PO_4)_2$ and $T_M = 82$ K for $Ba_2Cu(PO_4)_2$ characteristic of quasi-one-dimensional systems. The $\chi(T)$ data were excellently fitted by the spin susceptibility curve for the uniform $S = 1/2$ chain (plus temperature-independent and Curie–Weiss terms) with $g = 2.153(4)$ and $J/k_B = 143.6(2)$ K for $Sr_2Cu(PO_4)_2$ and $g = 2.073(4)$ and $J/k_B = 132.16(9)$ K for $Ba_2Cu(PO_4)_2$ (Hamiltonian $H = J\Sigma S_iS_{i+1}$). The similar J/k_B values were obtained from the specific heat data. No anomaly was observed on the specific heat from 0.45 to 21 K for both compounds indicating that the temperatures of long-range magnetic ordering, T_N, were below 0.45 K. $Sr_2Cu(PO_4)_2$ and $Ba_2Cu(PO_4)_2$ are an excellent physical realization of the $S = 1/2$ linear chain Heisenberg antiferromagnet with $k_BT_N/J < 0.34\%$ together with Sr_2CuO_3 ($k_BT_N/J \approx 0.25\%$) and γ-LiV_2O_5 ($k_BT_N/J < 0.16\%$). $Sr_2Cu(PO_4)_2$ and $Ba_2Cu(PO_4)_2$ were stable in air up to 1280 and 1150 K, respectively.

Keywords: Copper phosphate; Heisenberg antiferromagnet; One-dimensional system; Magnetic susceptibility; Specific heat; Thermal analysis

1. Introduction

The discovery of diverse cooperative quantum phenomena in different compounds has stimulated a search for new materials with low-dimensional magnetic sublattices. A variety of one- (1D) and two-dimensional (2D), as well as systems with intermediate dimensions, e.g., coupled chains or spin ladders, has been found and investigated [1].

The spin number and the geometry of the magnetic sublattice affect the ground state of quantum antiferromagnets (AFs). For example, spin singlet ground states with finite gaps to magnetic excited states have been found in 1D AF systems, e.g., $S = 1/2$ alternating bond chains [2,3], $S = 1/2$ two-leg ladders [4], and $S = 1$ chains (Haldane systems) [5]. The discovery of $CuGeO_3$ (spin Peierls) [6], $(VO)_2P_2O_7$ (alternating chains) [7], Y_2BaNiO_5 (Haldane) [8], $SrCu_2O_3$ [9,10], and $Sr_{14}Cu_{24}O_{41}$ (ladders) [11] in the past decades has continued to attract attention to 1D systems.

A uniform Heisenberg half-integer spin chain has a gapless spin excitation spectrum. The ground state is disordered because of strong quantum fluctuations. 1D gapless systems do not undergo three-dimensional (3D) magnetic ordering. However, real quasi-1D gapless systems exhibit long-range ordering (LRO) due to finite interchain interactions. For example, a $S = 5/2$ 1D system, $(CH_3)_4NMnCl_3$ (TMMC), has a 3D magnetic ordering at $T_N = 0.835$ K [12]. Sr_2CuO_3 was considered as an excellent physical realization of the $S = 1/2$ linear chain Heisenberg AF [13,14] because it has $T_N = 5.4$ K and the exchange coupling constant, J/k_B, of about 2200 ± 200 K [13] giving the ratio $k_BT_N/J \approx 0.25\%$. Another example of systems with the low k_BT_N/J ratio is γ-LiV_2O_5 ($k_BT_N/J < 0.16\%$) [1,15].

*Corresponding author. Fax: +81-774-38-3125.
E-mail address: belik@msk.kuicr.kyoto-u.ac.jp (A.A. Belik).

0022-4596/$ - see front matter © 2003 Elsevier Inc. All rights reserved.
doi:10.1016/j.jssc.2003.09.024

$Sr_2Cu(PO_4)_2$ [16] and $Ba_2Cu(PO_4)_2$ [17] crystallize in space group $C2/m$ (No. 12) with $a = 11.5155$ Å, $b = 5.0754$ Å, $c = 6.5749$ Å, and $\beta = 106.356°$ for the former and $a = 12.160$ Å, $b = 5.133$ Å, $c = 6.885$ Å, and $\beta = 105.42°$ for the latter. Cu^{2+} ions in the structures of these two compounds have a square-planar coordination. The CuO_4 polyhedra are connected with each other through two PO_4 groups forming infinite $[Cu(PO_4)_2]_\infty$ linear chains along the b direction as shown in Fig. 1. The Cu–Cu distance in the chain equals to the length of the b axis. A quasi-1D character of the structure of $Ba_2Cu(PO_4)_2$ was emphasized by Etheredge and Hwu [17]. These authors measured magnetic susceptibility of $Ba_2Cu(PO_4)_2$ at 4.7–300 K but they did not observe a maximum characteristic of the uniform $S = 1/2$ 1D Heisenberg chain, probably because of the large Curie–Weiss contribution coming from a poor sample quality.

In this work, we have studied properties of $Sr_2Cu(PO_4)_2$ and $Ba_2Cu(PO_4)_2$ by magnetic susceptibility and specific heat measurements. These compounds were shown to be another excellent physical realization of the quasi-1D Heisenberg chain with $k_BT_N/J < 0.34\%$. We have also investigated the thermal stability of $Sr_2Cu(PO_4)_2$ and $Ba_2Cu(PO_4)_2$ in air.

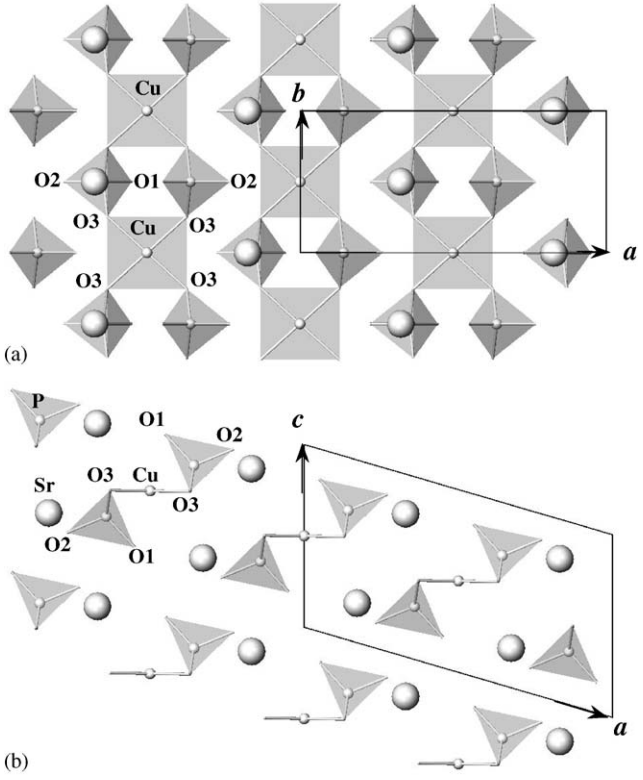

Fig. 1. Projections of the structure of $Sr_2Cu(PO_4)_2$ with (a) the c-axis perpendicular to this page and (b) the b-axis perpendicular to this page. $[Cu(PO_4)_2]_\infty$ linear chains are along the b direction. PO_4 and CuO_4 polyhedra are shown. Sr atoms are presented by big spheres.

2. Experimental section

$Sr_2Cu(PO_4)_2$ and $Ba_2Cu(PO_4)_2$ were prepared from stoichiometric mixtures of $SrCO_3$ (99.99%), $BaCO_3$ (99.9%), CuO (99.99%), and $NH_4H_2PO_4$ (99.8%) by the solid state method in alumina crucibles. The mixtures were heated very slowly from room temperature to 770 K, reground, and then allowed to react at 1150 K for $Sr_2Cu(PO_4)_2$ and at 1050 K for $Ba_2Cu(PO_4)_2$ for 200 h with five intermediate grindings. Both of the obtained samples were blue. X-ray powder diffraction (XRD) data collected with a RIGAKU RINT 2500 diffractometer (2θ range of 10–60°, a step width of 0.02°, and a counting time of 1 s/step) showed that $Sr_2Cu(PO_4)_2$ contained impurity of α-$Sr_2P_2O_7$ (0.8%), and $Ba_2Cu(PO_4)_2$ contained impurity of $Ba_3(PO_4)_2$ (0.2%). Mass fractions of impurities were estimated from scale factors refined in their Rietveld analyses.

Magnetic susceptibilities, χ, of $Sr_2Cu(PO_4)_2$ and $Ba_2Cu(PO_4)_2$ were measured on a DC SQUID magnetometer (Quantum Design, MPMS XL) between 2 and 400 K in applied fields of 100 Oe under both zero-field-cooled (ZFC) and field-cooled (FC) conditions. Specific heat capacities, C_p, were recorded between 0.45 and 21 K (on cooling) by a pulse relaxation method using a commercial calorimeter (Quantum Design PPMS).

Thermal stability of $Sr_2Cu(PO_4)_2$ and $Ba_2Cu(PO_4)_2$ was examined under air with a MacScience TG-DTA 2000 instrument. The samples were placed in Pt crucibles, heated, and then cooled with a rate of 10 K/min.

3. Results and discussion

Fig. 2 presents plots of χ (ZFC curves) against temperature, T, for $Sr_2Cu(PO_4)_2$ and $Ba_2Cu(PO_4)_2$. No notable difference was found between the curves measured under the ZFC and FC conditions. The $\chi(T)$ data exhibited a broad maximum at $T_M = 92$ K for $Sr_2Cu(PO_4)_2$ and $T_M = 82$ K for $Ba_2Cu(PO_4)_2$ which is characteristic of quasi-1D systems. In the temperature range of 3.2–400 K for $Sr_2Cu(PO_4)_2$ and 2–400 K for $Ba_2Cu(PO_4)_2$, the $\chi(T)$ data were fitted well by the equations:

$$\chi_{fit}(T) = \chi_0 + C_{imp}/(T - \theta_{imp}) + \chi_{chain}(T), \quad (1)$$

$$\chi_{chain}(T) = \frac{Ng^2\mu_B^2}{k_BT}\frac{0.25 + 0.14995x + 0.30094x^2}{1 + 1.9862x + 0.68854x^2 + 6.0626x^3}, \quad (2)$$

where $\chi_{chain}(T)$ is the Bonner–Fisher curve [2] parameterized by Estes et al. [18], $x = J/(2k_BT)$, N is Avogadro's number, μ_B is the Bohr magneton, k_B is Boltzmann's constant, g is the spectroscopic splitting

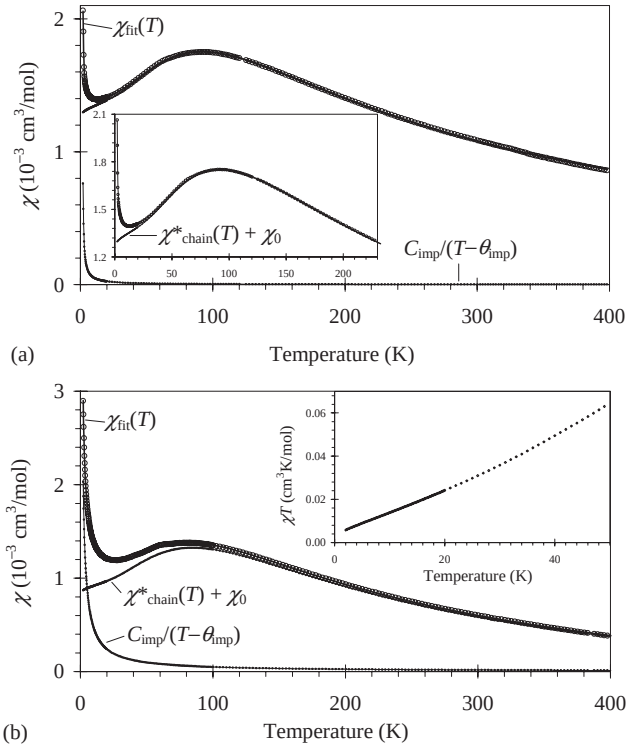

Fig. 2. Magnetic susceptibilities (o) against temperature, $\chi(T)$, for (a) $Sr_2Cu(PO_4)_2$ and (b) $Ba_2Cu(PO_4)_2$. Solid lines represent the fits by Eqs. (3) and (4), $\chi_{fit}(T)$. Solid lines with small dots are contributions of $\chi_0 + \chi^*_{chain}(T)$ and $C_{imp}/(T-\theta_{imp})$. Inset in (a) gives the enlarged fragment of this figure. Inset in (b) shows the χT versus T curve for $Ba_2Cu(PO_4)_2$ below 50 K.

Table 1
Fitted parameters for $\chi(T)$ and $C_p/T(T^2)$ of $Sr_2Cu(PO_4)_2$ and $Ba_2Cu(PO_4)_2$

Equation	Quantity	$Sr_2Cu(PO_4)_2$	$Ba_2Cu(PO_4)_2$
Eqs. (1) and (2)	Temperature range (K)	3.2–400	2–400
	χ_0 (cm^3 mol^{-1})	$-2.07(6)\times10^{-5}$	$-4.37(4)\times10^{-4}$
	C_{imp} (cm^3 K mol^{-1})	$2.21(5)\times10^{-3}$	$6.07(3)\times10^{-3}$
	θ_{imp} (K)	−3.18(15)	−0.88(2)
	g	2.152(4)	2.050(4)
	J/k_B (K)	146.4(2)	132.9(2)
	σ_{rms} (%)[a], R[b]	0.421, 1.68×10^{-5}	0.698, 4.66×10^{-5}
Eqs. (3) and (4)	Temperature range (K)	2–400	2–400
	χ_0 (cm^3 mol^{-1})	$-3.0(3)\times10^{-5}$	$-4.68(2)\times10^{-4}$
	C_{imp} (cm^3 K mol^{-1})	$4.54(6)\times10^{-4}$	$4.884(8)\times10^{-3}$
	θ_{imp} (K)	1.403(11)	−0.406(5)
	g	2.153(4)	2.073(4)
	J/k_B (K)	143.6(2)	132.16(9)
	σ_{rms} (%)[a], R[b]	0.472, 2.20×10^{-5}	0.355, 5.24×10^{-6}
Eq. (5)	Temperature range (K)	3–21	3–21
	γ (mJ K^{-2} mol^{-1})	37.2(5)	42.1(1.3)
	β_1 (mJ K^{-4} mol^{-1})	0.526(7)	1.10(2)
	β_2 (mJ K^{-6} mol^{-1})	$1.6(2)\times10^{-4}$	$-7(4)\times10^{-5}$

[a] $\sigma^2_{rms} = \frac{1}{N_p}\sum_{i=1}^{N_p}\left[\frac{(\chi(T_i)-\chi_{fit}(T_i))}{\chi(T_i)}\right]^2$ where N_p is the number of data points.

[b] $R = \frac{\sum_{i=1}^{N_p}(\chi(T_i)-\chi_{fit}(T_i))^2}{\sum_{i=1}^{N_p}(\chi(T_i))^2}$.

factor (g-factor), and J is the exchange constant with the Hamiltonian formulated as $H = J\Sigma S_i S_{i+1}$. The fitted parameters and measures of the quantity of fits (σ_{rms} and R) are given in Table 1.

The $\chi(T)$ data were taken in the temperature range corresponding to $0.01 < k_BT/J < 3.1$. It is known that at $k_BT/J < 0.25$, the Bonner–Fisher curve deviates from the recent calculations of spin susceptibility for the uniform $S = 1/2$ chain [14,19]. This may be the reason why the $\chi(T)$ data for $Sr_2Cu(PO_4)_2$ could not be fitted well by Eqs. (1) and (2) in the whole temperature range of 2–400 K (in this case, $\sigma_{rms} = 1.31\%$ and $R = 1.85\times10^{-4}$). The excellent fits in the whole temperature range were obtained using the equations:

$$\chi_{fit}(T) = \chi_0 + C_{imp}/(T-\theta_{imp}) + \chi^*_{chain}(T), \quad (3)$$

$$\chi^*_{chain}(T) = \frac{Ng^2\mu_B^2}{4k_BT}\frac{1+\sum_{n=1}^{5}N_n/t^n}{1+\sum_{n=1}^{6}D_n/t^n}, \quad (4)$$

where $\chi^*_{chain}(T)$ is the spin susceptibility curve of the uniform $S = 1/2$ chain parameterized by Johnston et al. (Eqs. (50) in Ref. [19]), $t = k_BT/J$, $N_1 = -0.053837836$, $N_2 = 0.097401365$, $N_3 = 0.014467437$, $N_4 = 0.0013925193$, $N_5 = 0.00011393434$, $D_1 = 0.44616216$, $D_2 = 0.32048245$, $D_3 = 0.13304199$, $D_4 = 0.037184126$, $D_5 = 0.0028136088$, $D_6 = 0.00026467628$. The fitted parameters and σ_{rms} and R are listed in Table 1. The magnetic susceptibilities calculated with Eqs. (3) and (4), $\chi_{fit}(T)$, are plotted on Fig. 2. The g and J/k_B parameters for $Sr_2Cu(PO_4)_2$ and $Ba_2Cu(PO_4)_2$ obtained from Eqs. (1) and (2) and from Eqs. (3) and (4) were similar to each other.

The second term in Eqs. (1) and (3) is related to the presence of impurities or defects with an impurity Curie constant C_{imp} and Weiss constant θ_{imp}, which gives rise to a low-temperature upturn in $\chi(T)$. The C_{imp} values correspond to 0.05% of free spins in $Sr_2Cu(PO_4)_2$, and 0.5% in $Ba_2Cu(PO_4)_2$. $Ba_2Cu(PO_4)_2$ was prepared at the lower temperature than $Sr_2Cu(PO_4)_2$. $Ba_2Cu(PO_4)_2$ had also the worse crystallinity than $Sr_2Cu(PO_4)_2$ as indicated by the line widths on the XRD patterns. It means that a larger number of defects was presented in $Ba_2Cu(PO_4)_2$ and the length of the Cu chains in $Ba_2Cu(PO_4)_2$ was shorter than that in $Sr_2Cu(PO_4)_2$. It

may explain why C_{imp} in $Ba_2Cu(PO_4)_2$ was larger than that in $Sr_2Cu(PO_4)_2$.

Note that relatively large J/k_B values were obtained for $Sr_2Cu(PO_4)_2$ and $Ba_2Cu(PO_4)_2$ taking into account the fact that the exchange interactions are transferred through PO_4 tetrahedra. A comparable exchange constant ($J_1/k_B = 136$ K) was assigned to the V–V interaction transferred via the PO_4 groups in $(VO)_2P_2O_7$ [20].

In the work of Etheredge and Hwu [17], the authors observed the increase of the χT values below 20 K for $Ba_2Cu(PO_4)_2$. This feature on the χT versus T curve was suggested to be caused by a possible antiferro-to-ferroelecrtic transition. Our data plotted as χT versus T showed no anomaly at low temperatures for $Ba_2Cu(PO_4)_2$ (see the inset of Fig. 2b) indicating the absence of the proposed magnetic phase transition.

Specific heat data were taken at zero field to investigate magnetism of $Sr_2Cu(PO_4)_2$ and $Ba_2Cu(PO_4)_2$ in more details. Fig. 3 shows the total specific heat divided by temperature, C_p/T, plotted against temperature, T, and temperature squared, T^2. The C_p/T values were almost constant below 2 K (see the inset of Fig. 3a). The slight upturn observed at very low temperatures

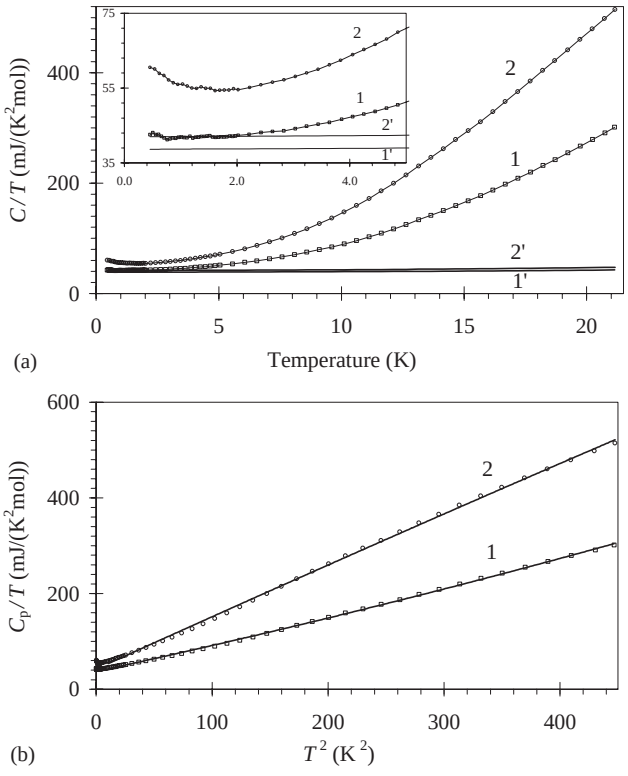

Fig. 3. Total specific heat divided by temperature, C_p/T, plotted against (a) T and (b) T^2 for $Sr_2Cu(PO_4)_2$ (1) and $Ba_2Cu(PO_4)_2$ (2). Thin solid lines between experimental points are drawn for the eye in (a). Thick solid lines in (a) are the calculated magnetic specific heat divided by temperature, $(C_m/T)_{calc}$, for $Sr_2Cu(PO_4)_2$ (1′) and $Ba_2Cu(PO_4)_2$ (2′). Inset in (a) shows the enlarged fragment of this figure. Solid lines in (b) represent the fits by Eq. (5).

(especially for $Ba_2Cu(PO_4)_2$) can be attributed to the vicinity of the 3D LRO transitions.

Because the present compounds are insulators, specific heat data consist of the magnetic and lattice components. At low temperatures, the magnetic specific heat divided by temperature, C_m/T, for the $S = 1/2$ AF uniform Heisenberg chain is known to be constant and equal to $(2/3)Nk_B^2/J = 5543.14(k_B/J)$. The initial deviation from this constant value is positive and approximately quadratic in T [19]. The lattice contribution can be expressed as $C_l = \beta_1 T^3 + \beta_2 T^5$. Therefore, the experimental $C_p/T(T^2)$ data can be fitted by the equation

$$C_p/T = \gamma + \beta_1 T^2 + \beta_2 T^4, \tag{5}$$

where $\gamma = C_m/T$

The calculated C_m/T curves, $(C_m/T)_{calc}$, for $Sr_2Cu(PO_4)_2$ and $Ba_2Cu(PO_4)_2$ are plotted on Fig. 3a. For our calculations, we used Eqs. (54) of Ref. [19] and the J/k_B parameters determined from the $\chi(T)$ data (Eqs. (3) and (4)):

$$C_m(T) = \frac{3Nk_B}{16t^2}\frac{1+\sum_{n=1}^{6}N_n/t^n}{1+\sum_{n=1}^{9}D_n/t^n} - a_1 t \sin\left(\frac{2\pi}{a_2+a_3 t}\right)e^{-a_4 t} - a_5 t\, e^{-a_6 t}, \tag{6}$$

where $t = k_BT/J$ and numerical values of the coefficients (N_1-N_6, D_1-D_9, and a_1-a_6) for C_m can be found in Ref. [19].

The $(C_m/T)_{calc}$ values were notably smaller than the experimental C_p/T values even at temperatures below 2 K, where the lattice contribution should be negligible. Such difference can be explained by the vicinity to T_N that gives an additional contribution to C_p. For $Ba_2Cu(PO_4)_2$, the difference between C_p/T and $(C_m/T)_{calc}$ below 2 K is larger than that for $Sr_2Cu(PO_4)_2$. This fact is in accordance with the larger upturn of C_p/T at the low temperatures for $Ba_2Cu(PO_4)_2$ than that for $Sr_2Cu(PO_4)_2$ suggesting that T_N for $Ba_2Cu(PO_4)_2$ is larger than T_N for $Sr_2Cu(PO_4)_2$.

For the reason described above, we fitted the $C_p/T(T^2)$ data by Eq. (5) above 3 K, i.e., in the temperature range corresponding to $0.02 < k_BT/J < 0.16$. The fitted parameters are presented in Table 1. The γ values correspond to J/k_B of 149(2) K for $Sr_2Cu(PO_4)_2$ and 132(4) K for $Ba_2Cu(PO_4)_2$. The values of β_1 give a Debye temperature, $\Theta_D = (234Nk_B/\beta_1)^{1/3}$, of 155 K for $Sr_2Cu(PO_4)_2$ and 121 K for $Ba_2Cu(PO_4)_2$. The J/k_B parameters for $Sr_2Cu(PO_4)_2$ and $Ba_2Cu(PO_4)_2$ obtained from the magnetic susceptibility and specific heat data were in good agreement with each other. Note that if we take the C_p/T values at 2 K as the γ values, we will obtain $J/k_B = 133$ K for $Sr_2Cu(PO_4)_2$ and $J/k_B = 102$ K for $Ba_2Cu(PO_4)_2$.

No anomaly characteristic of magnetic LRO was observed on the specific heat data. This fact gives us evidence to believe that $Sr_2Cu(PO_4)_2$ and $Ba_2Cu(PO_4)_2$ do not undergo magnetic LRO transitions down to 0.45 K. In addition, the C_p/T values were almost constant at low temperatures and approximately corresponded to the expected J/k_B parameters. This fact also confirms the good 1D character of the present compounds. Thus, $Sr_2Cu(PO_4)_2$ and $Ba_2Cu(PO_4)_2$ are other examples of an excellent physical realization of the $S = 1/2$ linear chain Heisenberg AF with $k_BT_N/J < 0.34\%$ together with the well known Sr_2CuO_3 ($k_BT_N/J \approx 0.25\%$) [13,14] and γ-LiV_2O_5 ($k_BT_N/J < 0.16\%$) [1,15].

To study the thermal stability, we heated $Sr_2Cu(PO_4)_2$ up to 1293 and 1333 K, and $Ba_2Cu(PO_4)_2$ up to 1133, 1183, and 1263 K (Fig. 4) and then analyzed the products by XRD. $Sr_2Cu(PO_4)_2$ heated up to 1293 K was green and the phase composition was not possible to identify except for small amount of $Sr_3Cu_3(PO_4)_4$. $Sr_2Cu(PO_4)_2$ melted when it was heated up to 1333 K. Thus, our differential thermal analysis (DTA) data showed that $Sr_2Cu(PO_4)_2$ was stable in air up to 1280 K (Fig. 4a). $Ba_2Cu(PO_4)_2$ heated up to 1133 K was blue and the phase composition was not changed. When $Ba_2Cu(PO_4)_2$ was heated up to 1183 K, it was grey-blue and reflections due to unknown impurities appeared on the XRD pattern in addition to the reflections of the main phase $Ba_2Cu(PO_4)_2$. Phase composition was not possible to identify (except for small amount of a phase isotypic with $Ba_2Ni(PO_4)_2$) when $Ba_2Cu(PO_4)_2$ was heated up to 1263 K. In the last case, the sample was green. Thus, our DTA data evidenced that $Ba_2Cu(PO_4)_2$ was stable in air up to 1150 K (Fig. 4b). This temperature is higher than the decomposition temperature (1068–1083 K) reported for $Ba_2Cu(PO_4)_2$ in the literature [17].

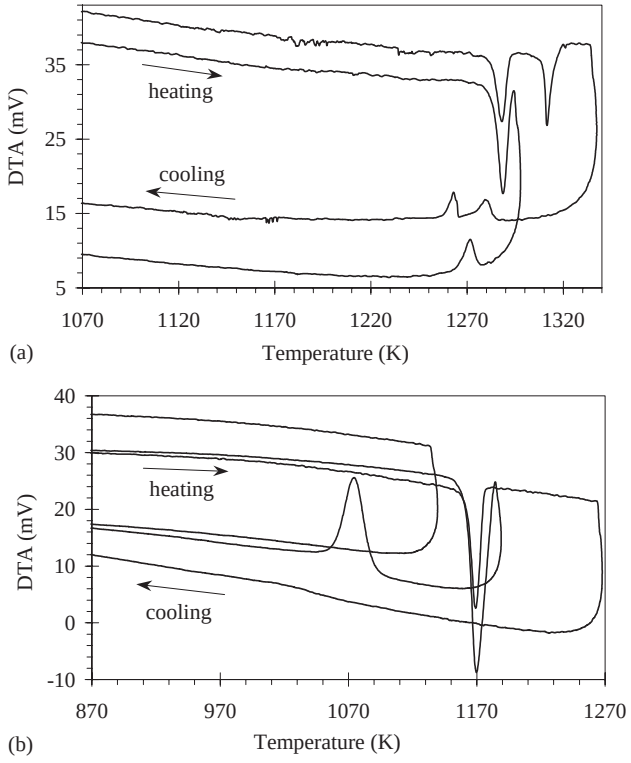

Fig. 4. DTA curves for (a) $Sr_2Cu(PO_4)_2$ and (b) $Ba_2Cu(PO_4)_2$.

In conclusion, we characterized quasi-1D $Sr_2Cu(PO_4)_2$ and $Ba_2Cu(PO_4)_2$ by magnetic susceptibility, specific heat, and thermal analysis. From the magnetic susceptibility data, we determined the exchange coupling constants between copper atoms ($J/k_B = 143.6$ K for $Sr_2Cu(PO_4)_2$ and $J/k_B = 132.2$ K for $Ba_2Cu(PO_4)_2$) which were consistent with the specific heat data. The specific heat data proved both compounds to be good quasi-1D systems with the ratio k_BT_N/J below 0.34%.

Acknowledgments

The authors express their thanks to the Ministry of Education, Culture, Sports, Science and Technology, Japan, for Grants-in-Aid No. 12CE2005, for COE Research on Elements Science (No. 13440111 and No. 14204070), and for 21COE on Kyoto Alliance for Chemistry.

References

[1] Y. Ueda, Chem. Mater. 10 (1998) 2653.
[2] J.C. Bonner, M.E. Fisher, Phys. Rev. 135 (1964) A640.
[3] (a) J.C. Bonner, H.W.J. Blöte, J.W. Bray, I.S. Jacobs, J. Appl. Phys. 50 (1979) 1810;
(b) J.C. Bonner, H.W.J. Blöte, Phys. Rev. B 25 (1982) 6959.
[4] E. Dagotto, T.M. Rice, Science 271 (1996) 618.
[5] F.D.M. Haldane, Phys. Rev. Lett. 50 (1983) 1153.
[6] M. Hase, I. Terasaki, K. Uchinokura, Phys. Rev. Lett. 70 (1993) 3651.
[7] M. Azuma, T. Saito, Y. Fujishiro, Z. Hiroi, M. Takano, F. Izumi, T. Kamiyama, T. Ikeda, Y. Narumi, K. Kindo, Phys. Rev. B 60 (1999) 10145.
[8] J. Darriet, L.P. Regnault, Solid State Commun. 86 (1993) 409.
[9] (a) Z. Hiroi, M. Azuma, M. Takano, Y. Bando, J. Solid State Chem. 95 (1991) 230;
(b) M. Azuma, Z. Hiroi, M. Takano, K. Ishida, Y. Kitaoka, Phys. Rev. Lett. 73 (1994) 3463.
[10] M. Azuma, M. Takano, R.S. Eccleston, J. Phys. Soc. Jpn. 67 (1998) 740.
[11] R.S. Eccleston, M. Uehara, J. Akimitsu, H. Eisaki, N. Motoyama, S. Uchida, Phys. Rev. Lett. 81 (1998) 1702.
[12] K. Takeda, T. Koike, T. Tonegawa, I. Harada, J. Phys. Soc. Jpn. 48 (1980) 1115.
[13] (a) N. Motoyama, H. Eisaki, S. Uchida, Phys. Rev. Lett. 76 (1996) 3212;
(b) A. Keren, L.P. Le, G.M. Luke, B.J. Sternlieb, W.D. Wu, Y.J. Uemura, S. Tajima, S. Uchida, Phys. Rev. B 48 (1993) 12926.

[14] D.C. Johnston, in: K.H.J. Buschow (Ed.), Handbook of Magnetic Materials, Vol. 10, Elsevier Science, Amsterdam, 1997, pp. 1–237.
[15] N. Fujiwara, H. Yasuoka, M. Isobe, Y. Ueda, S. Maegawa, Phys. Rev. B 55 (1997) R11945.
[16] A.A. Belik, A.P. Malakho, B.I. Lazoryak, S.S. Khasanov, J. Solid State Chem. 163 (2002) 121.
[17] K.M.S. Etheredge, S.-J. Hwu, Inorg. Chem. 35 (1996) 1474.
[18] W.E. Estes, D.P. Gavel, W.E. Hatfield, D.J. Hodjgson, Inorg. Chem. 17 (1978) 1415.
[19] D.C. Johnston, R.K. Kremer, M. Troyer, X. Wang, A. Klümper, S.L. Bud'ko, A.F. Panchula, P.C. Canfield, Phys. Rev. B 61 (2000) 9558.
[20] J. Kikuchi, K. Motoya, T. Yamauchi, Y. Ueda, Phys. Rev. B 60 (1999) 6731.